



TRANSVERSAL FLOW AND HEAT TRANSFER OF TWO CYLINDERS WITH A FLAPPING REED BETWEEN THEM

Zhiyun Wang^{*}, Ziqing Wang, Mo Yang

School of Energy and Power Engineering, University of Shanghai for Science and Technology, Shanghai, 200093, China

ABSTRACT

This paper presents a two-dimensional fluid-structure interaction numerical simulation of fluid flow over two horizontal heat exchange cylinders affected by a flapping reed in a domain. The reed is a thin flexible sheet made of elastic material with one end fixed on the trailing edge of the upstream cylinder. The effects of the reed length and the cylinder spacing on the periodic oscillations of the reed, the flow field and the heat transfer of the downstream cylinder. The results show that the oscillation of the reed in this paper is a single-period oscillate model. Compared to the case of cylinder without any measurement of heat transfer enhancement (clean cylinder), the heat transfer performance of the cylinder with the reed could be enhanced under certain conditions. For the case of the cylinder spacing $S^*=1.5$, as the length of the reed increases, the heat transfer of the downstream cylinder increases by up to 14% compared to the clean cylinder, while the domain resistance coefficient is almost unchanged. For the cases of cylinder spacing $S^*=2.0$, as the length of the reed increases, the heat transfer of the downstream cylinder gradually decreases, but the domain resistance coefficient gradually increases to 12%.

Keywords: *fluid-structure interaction, heat and mass transfer, transversal flow, cylinders, numerical simulation*

1. INTRODUCTION

In recent years, obtaining higher heat transfer efficiency through enhanced heat transfer technology has become a hot issue in heat exchanger. According to Bergles' (1999) classification method of heat transfer enhancement by convection, it can be roughly divided into the passive enhancement technology and the active enhancement technology. The active type must rely on external power, such as mechanical force or electromagnetic force, while the passive type does not need to use other forms of power besides the power required to transport the fluid medium. Therefore, compared with the active type, the passive type reduces cost consumption and enhances equipment reliability (Beskok *et al.*, 2012; Pourgholam *et al.*, 2015).

Heat transfer augmentations through the use of the passive type that enhance flow mixing and reduce mechanical loss have been the subject of much research effort. According to their movability, the passive enhancement technology can be divided into the fixed type and the flapping type. In the process of enhancing heat transfer, the flapping type produces deformation and displacement under the action of fluid. In various studies (Fiebig *et al.*, 1993; Facchinetti *et al.*, 2004; Yoo *et al.*, 2002; Song and Wang, 2013), scholars had conducted in-depth studies on the enhancement of heat transfer performance of the fixed type under different shapes and tube spacing. About the flapping type (Li *et al.*, 2018; Gallegos *et al.*, 2017; Lee *et al.*, 2017; Lee *et al.*, 2018; Chen *et al.*, 2020; Khanafer *et al.*, 2010), researchers have made great efforts. They studied the influence of different shapes, different placement forms, and different physical parameters of the flapping reed on the heat transfer performance of the channel. Compared with the fixed type, the flapping type heat transfer performance is better, and the channel pressure loss is smaller. Instead of modifying the channel surface, flapping vortex generator made of elastic material can be placed in the

existing channel directly. Therefore, the fluid-structure coupling passive flapping reed enhanced heat transfer has become a hot topic in many engineering fields (Facchinetti *et al.*, 2004).

In summary, most of the previous studies focused on the influence of the flapping reed on the heat transfer of the channel, but did not study its influence on the heat transfer of the heat exchanger tubes. Therefore, this article is based on the enhanced heat transfer of the flapping reed. Take the variation of reed length and the change of the cylinder spacing as the research focus. By means of two-dimensional fluid-structure interaction (FSI) numerical simulation, research on the heat transfer enhancement and the fluid flow characteristics.

2. PROBLEM STATEMENT AND MATHEMATICAL MODEL

2.1 Physical Model

The two-dimensional physical model is shown schematically in Fig. 1. The fluid enters the domain at the left boundary with a uniform velocity U and low temperature T_{in} and then flow across two cylinders with higher temperature T_{wall} . There would be the heat exchange between the fluid and the cylinders due to the temperature difference in the domain. The diameter of the cylinder is D and the length of the domain $C_L=12D$. With the set of the domain height $C_H=4.1D$ and the upper and lower boundaries walls are set to be symmetrical conditions. The setting is intentionally non-symmetric to prevent the dependence of the onset of any possible oscillation on the precision of the computation. The influence of upper and lower boundary to the flow and heat transfer can be ignored in this model (Khan *et al.*, 2006). A flexible sheet is installed as the reed with one end fixed on the trailing edge of the upstream cylinders. The length of reed is L . The distance between the two cylinders is S . The right boundary is set to a constant pressure and

^{*}Corresponding author. Email: wangzhiyun@usst.edu.cn

far enough from the cylinders. The surfaces of the two cylinders are no slip boundary condition. The surface of the reed is adiabatic and the thickness of it is H which is used only for the calculation of the solid inner stress.

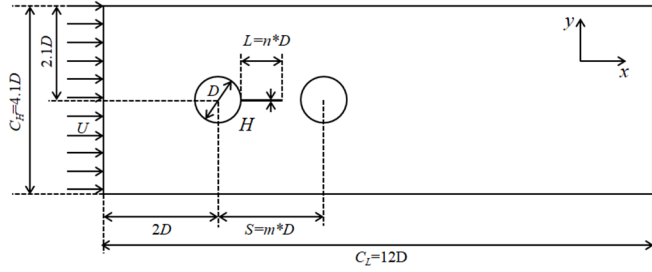


Fig. 1 Physical model

2.2 Mathematical Model

It is assumed in this investigation that the flow is two-dimensional, steady and incompressible. The FSI model calculation region contains the fluid domain and the solid domain. An arbitrary Lagrangian–Eulerian formulation was adopted to describe the fluid motion. Furthermore, the governing equations for the fluid domain are the continuity and Navier–Stokes equations. Thus, the Navier–Stokes equations are described in tensor form as:

$$\rho_f \frac{\partial u_i}{\partial t} + \rho_f u_{i,j} (u_j - \hat{u}_j) = \sigma_{ij,j} + \rho_f f_i \quad (1)$$

$$u_{i,i} = 0$$

Where ρ_f is the fluid density, u_i is the velocity tensor, t is the time, \hat{u}_j is the moving velocity of the solid region and indices indicate vector components and differentiation in index (notation), $\sigma_{ij,j}$ is the stress tensor and f_i is the body force per unit mass. For incompressible fluids, the principle of conservation of thermal energy is expressed by:

$$\rho_f C_p \left(\frac{\partial T}{\partial t} + u_i T_{,i} \right) = (\lambda_f T_{,i})_{,i} \quad (2)$$

Where T is the temperature, λ_f is the thermal conductivity of the fluid, and C_p is the specific heat at constant pressure. In addition, the governing equation for the solid domain of the FSI model can be described by the following equation:

$$\rho_s \ddot{d}_i = \bar{\sigma}_{ij,j} + \rho_s \bar{f}_i \quad (3)$$

Where ρ_s is the flapping reed density, $\bar{\sigma}_{ij,j}$ is the solid Cauchy stress tensor, \bar{f}_i is the externally applied body force vector at time t and \ddot{d}_i represents the acceleration of the solid domain.

While the inlet and outlet boundary conditions implemented in this investigation are summarized as follows:

$$x = 0: u = U, v = 0, T = T_{in}$$

$$x = L: \frac{\partial u}{\partial x} = \frac{\partial v}{\partial x} = \frac{\partial T}{\partial x} = 0 \quad (4)$$

About the top and bottom thermal boundaries and the thermal boundary conditions along the flapping reed are given by:

$$y = 0, C_H \text{ and } 0 \leq x \leq C_L: u = v = \frac{\partial T}{\partial y} = 0 \quad (5)$$

The thermal boundaries on the surface of both cylinders are as follows:

$$T = T_{wall} \quad (6)$$

The final set of boundary conditions is the FSI interfaces such that the conditions of displacement compatibility and traction equilibrium along the structure–fluid interfaces must be satisfied as follows respectively:

$$\begin{aligned} d_f &= d_s \\ \sigma_f &= \sigma_s \end{aligned} \quad (7)$$

Where d_f and d_s are the displacements, σ_f and σ_s are the tractions of the fluid and the solid.

2.3 Dimensionless Parameter Definition

The problem is then described by 7 dimensionless parameters:

$$\begin{aligned} S^* &= \frac{S}{D}, L^* = \frac{L}{D}, H^* = \frac{H}{D}, \\ \rho^* &= \frac{\rho_s}{\rho_f}, E^* = \frac{E}{\rho_f U^2}, \nu_s = 0.4, \\ \text{Re} &= \frac{UD}{\nu_f} \end{aligned} \quad (8)$$

Where the superscript * represents non-dimensional parameters. H^* represents the non-dimensional thickness of the reed, which is a constant and the value is 0.2. The elasticity of the solid material is characterized by the Poisson ratio ν_s and E^* , which are fixed at 0.4 and 2.5 respectively in this article. The Reynolds number used in this study is fixed at 200 for all cases. The heat transfer performance is evaluated by Nu number, which is defined as follows:

$$\begin{aligned} \text{Nu}_{ave} &= \frac{\bar{h}D}{\lambda} \\ \text{Nu}_\alpha &= \frac{h_\alpha D}{\lambda} \end{aligned} \quad (9)$$

Where Nu_{ave} and Nu_α are the average heat transfer and local transfer performance of the downstream cylinder. In the expression, \bar{h} and h_α are the average convection heat transfer coefficient and local convection heat transfer coefficient of the downstream cylinder. They are summarized as follows:

$$\begin{aligned} \bar{h} &= \frac{1}{2\pi} \int_0^{2\pi} h \alpha d\alpha \\ h_\alpha &= \frac{-\lambda \frac{\partial T}{\partial n}}{T_{wall} - T_{in}} \end{aligned} \quad (10)$$

Where α is the angle between the calculation point on the cylinder and the direction of the incoming flow. The resistance coefficient is used to evaluate the pressure drop of the fluid in all condition, which is as follows:

$$C_D = \frac{2\Delta p}{\rho_f U^2 D} \quad (11)$$

In this expression, Δp is the domain pressure drop. The dimensionless amplitude of the free end of the flapping reed is shown as:

$$A_y^* = \frac{A_y}{D} \quad (12)$$

Where A_y is the maximum amplitude of the free end of the flapping reed in the direction perpendicular to the incoming fluid.

2.4 Numerical Method

Simulation method used in this article is finite element formulation based on the Galerkin method, which was employed to solve the governing equations of a FSI model. According to the boundary conditions in Eqs. (4) and (8), the finite element method was used to discretize the continuity and momentum formulas. These equations are weighted with the virtual quantities of pressure and velocities. A variable grid-size system was employed to capture the rapid changes in the dependent variables especially near the wall where the major gradients occur inside the boundary layer. In addition, the Newton–Raphson method was used to solve the discretized equations for the fluid and solid domain. The time step size of 0.005s was used until periodic convergence solution is achieved.

3. VERIFICATION NUMERICAL METHOD AND GRID INDEPENDENCE

3.1 Numerical Simulation Method Verification

The commercial software COMSOL Multiphysics is employed to simulate the FSI process. In order to verify the numerical method, the problems shown in Fig.2 are simulated and result of A_y^* and C_D are compared with those reported by Turek *et al.* (2006) and Tian *et al.* (2014). In Fig.2, the fluid enters the domain at the left boundary with a parabolic velocity U which average is \bar{U} . The upper and lower boundaries are the walls. The dimensionless length of the physical model is shown in the Fig. 2.

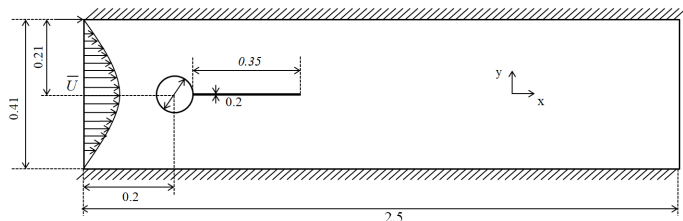


Fig. 2 Physical model of verify numerical method

The detail of comparison is listed in Table 1. It can be seen that the results obtained by the numerical method employed in this paper are consistent with the previous researches, which indicate that the numerical simulation method used in this paper is feasible.

Table 1 Verification of A_y^* and C_D results

Physical parameters	Comparative case	A_y^*	C_D
$\rho^*=10$ $Re=100$ $E^*=1.4 \times 10^3$	Turek	0.83	4.13
	Tian	0.78	4.11
	Present result	0.7836	4.1205
$\rho^*=1$ $Re=200$ $E^*=1.4 \times 10^3$	Turek	0.36	2.30
	Tian	0.32	2.16
	Present result	0.3189	2.1723

3.2 Grid independence verification

The structured meshing is used for the physical model and the grid near the cylinders is densified. Different grid size of 38000, 46800, 65050, 81050, 102050, 115000, 122000, 136050 and 140600 are employed respectively for the case of $S^*=2.0$ and $L^*=0.7$. Figure 3 shows a diagram of A_y^* and Nu_{ave} under different grids size. Grid independence is achieved within 0.06% in A_y^* number and 0.18% in Nu_{ave} with grid size of 122,000 which will be used for the follow-up calculations.

4. RESULTS AND DISCUSSION

$S^*=1.5$ and 2.0 are considered in this paper, since they represent the typical spacing adapt in industry that may cause stagnation vortexes between cylinders and would lead to heat transfer weakness (Marsters, 1972). The set of flapping reed between two cylinders may be adverse to the formation of stable stagnation vortexes.

4.1 Effects of the Length of Reed Under $S^*=1.5$

When $S^*=1.5$ and the length of the reed $L^*=0.10, 0.25, 0.30, 0.35$ and 0.40 is investigated. Under this condition, the reed is the single-period flapping model (Connell *et al.* 2007). Figure 4 shows the A_y^* change with time under the limit condition of $L^*=0.10$ and 0.40 and the Fourier analysis results. There is an obvious peak at a certain frequency, while it can be inferred that the flapping model of reed is a self-sustaining periodic oscillation.

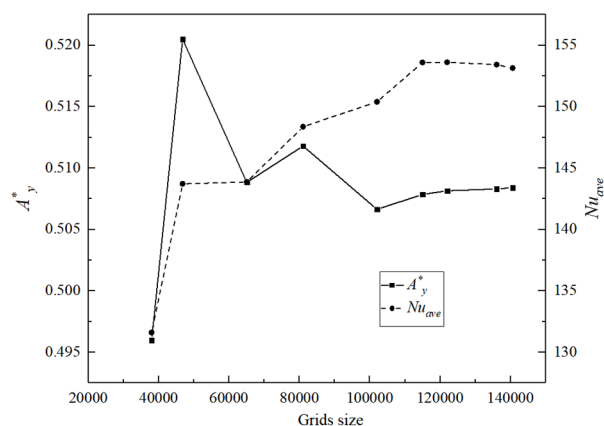


Fig. 3 A_y^* and Nu_{ave} under different grids size

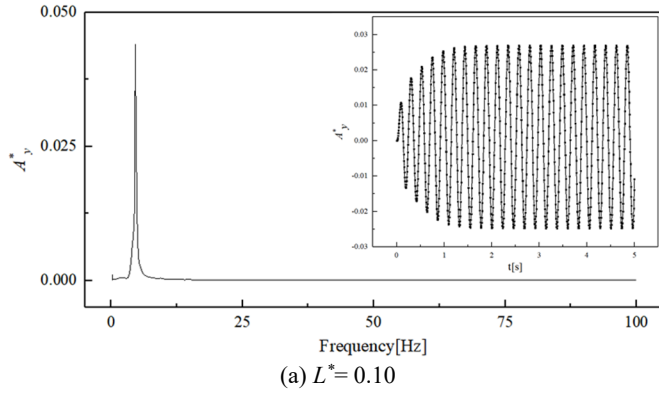
The percentage change rate of downstream cylinder Nu_{ave} and the domain C_D under different reed length are compared with those of the clean cylinder and shown in Fig. 5. When the L^* is increased from 0 to 0.25, Nu_{ave} and C_D hardly change. As L^* further increases to 0.40, the percentage change rate of Nu_{ave} is reaches up to 12%. Simultaneously, C_D changes little.

Figure 4 shows amplitude of the free end of the reed A_y in the direction perpendicular to the mainstream is stable after $t=2.5s$ and $2.9s$, respectively and the oscillation of the reed is single periodic. Therefore, it is possible to simplify the analysis of Nu_α on the downstream cylinder, and only analyze the upper half of the cylinder. All cases in this article, after 7 periods of stable oscillation of the reed, the heat transfer becomes stable, and the time average Nu_α is calculated from 8 to 12 oscillation periods. α ($0^\circ \leq \alpha \leq 180^\circ$) is the angle between the direction of the incoming flow and the point on the surface of the cylinder, as shown in Fig. 6. Nu_α at $\alpha=0^\circ$ is lower than other place. It is because that the distance between the cylinders is small which causes a flow stagnation point at the leading edge point of the downstream cylinder. As α increase to 50° , Nu_α gradually increases, and then keeps a relative higher value until $\alpha \leq 80^\circ$. As the results of the twin vortexes between the cylinders enhance fluid turbulence and heat transfer. At $50^\circ \leq \alpha \leq 125^\circ$, the heat transfer weakens due to the boundary layer gradually thickens. Along with α increase up to 180° , fluid departs from the surface of the cylinder which enhanced heat transfer. Results in local Nu_α rebounded.

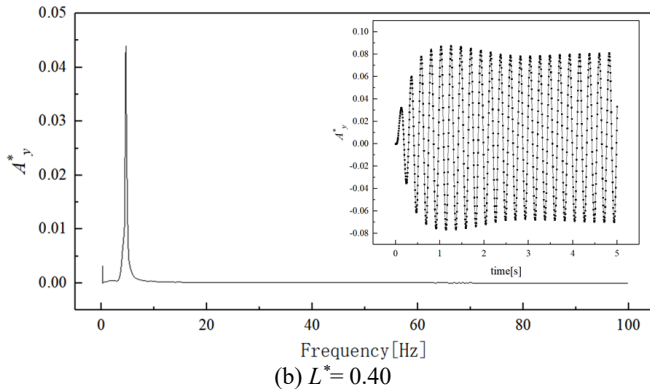
To quantify the difference, this paper selects the representative conditions when $L^*=0.25$ and 0.40 . Comparing the condition when $L^*=0$ and 0.25 , it is obviously that Nu_α has a certain increase in the range of $0^\circ \leq \alpha \leq 7^\circ$, result of the flapping of the reed destroys the front stagnation point of the downstream cylinder. While in the range of $7^\circ \leq \alpha \leq 180^\circ$ the oscillating motion has almost no effect on the Nu_α , due to the shorter length of the reed which has little effect on the vortex between the cylinders and has almost no effect on the Nu_α . Comparing of $L^*=0$ and 0.40 shown in Fig.6, Nu_α with the reed is obviously higher than Nu_α of the clean cylinder at $0^\circ \leq \alpha \leq 18^\circ$ and $113^\circ \leq \alpha \leq 180^\circ$. Within the range of $18^\circ \leq \alpha \leq 113^\circ$, there is not much difference.

The reed flapping for one period under the conditions of $L^*=0$ and 0.40 the temperature gradient map are shown in Fig. 7. At $t=4.04s, 4.09s$ and $4.15s$, during $0^\circ \leq \alpha \leq 7^\circ$ due to the small distance between the cylinders, there is a stable twin vortex in the flow between the cylinders, while the left end of the downstream cylinder is the stagnation point. The flapping reed thins or destroys the thermal boundary layer on the left end of the downstream cylinder, which also increases the chaos of the fluid between the cylinders, increases the temperature gradient, and

enhances the heat transfer performance. Fig. 8 shows the vorticity diagrams under the same condition. Due to the flapping of the reed, the vorticity at A and B marked in Fig. 8 is stronger than the vortex at same position of the clean cylinder. As the result of the increased vorticity, the vortices on the upper and lower sides of the downstream cylinder are squeezed and become smaller. This phenomenon brings the flow dead zone reduction and the mixing of the fluid of mainstream and the fluid at the downstream cylinder surface. Ultimately, heat transfer is enhanced.



(a) $L^* = 0.10$



(b) $L^* = 0.40$

Fig. 4 A_y^* change with time and the Fourier analysis results

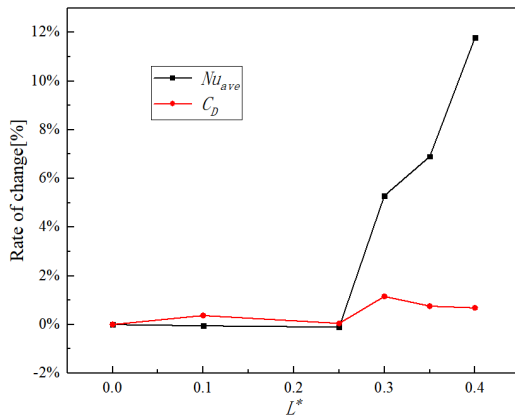


Fig. 5 Under $S^*=1.5$ trend of Nu_{ave} and C_D when the L^* changes

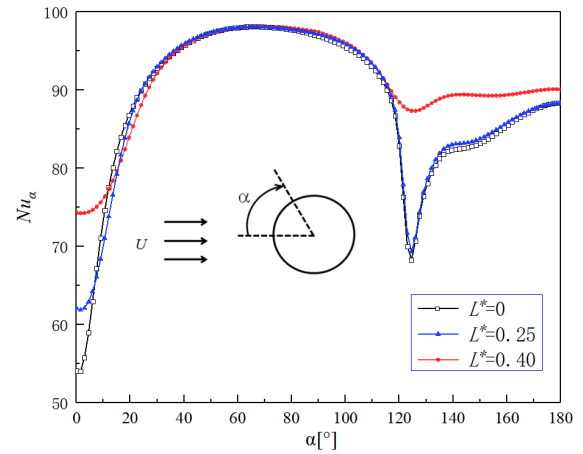


Fig. 6 $L^* = 0, 0.25$ and 0.40 Variation trend of Nu_α with α

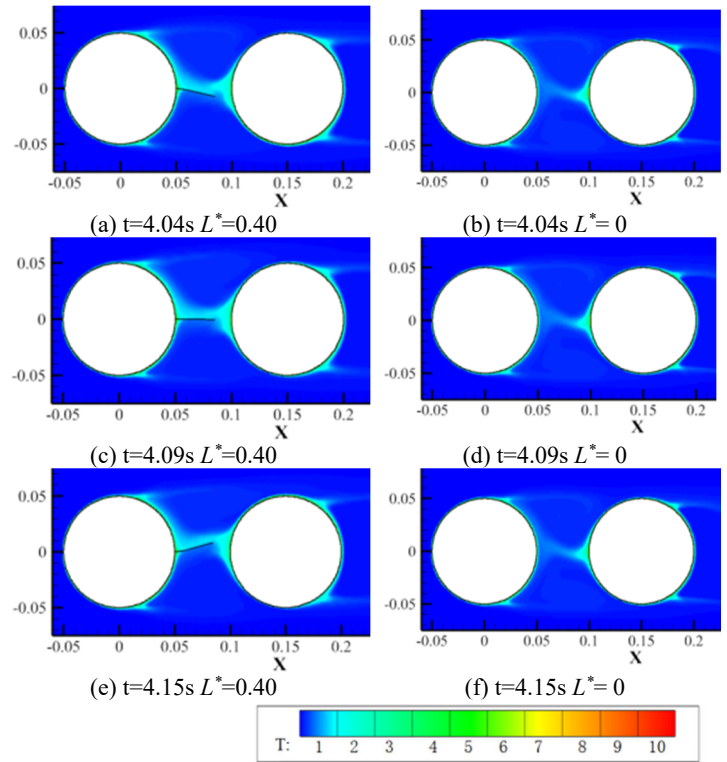


Fig. 7 $L^* = 0$ and 0.40 temperature gradient at different times

4.2 Effects of the Length of Reed Under $S^*=2.0$

Under the condition of $S^*=2.0$, along with the length of the reed L^* changes, Nu_{ave} and C_D have a completely different trend from previous case. The analysis method is the same as $S^*=1.5$. As shown in Fig. 9, the reed flapping, it also can be inferred that the flapping model of reed is a self-sustaining periodic oscillation. Fig. 10 shows under $S^*=2.0$ change the percentage change rate of Nu_{ave} and C_D when the L^* changes, obviously contrary to the previous trend. Fig. 10 shows that the reed length increases from 0 to $0.25D$, the percentage change rate of Nu_{ave} increases by 10.58%, and the C_D hardly changes. As the length of the reed further increases, the Nu_{ave} decreases until no difference from the clean cylinder. Simultaneously, C_D significantly increases to about 12%.

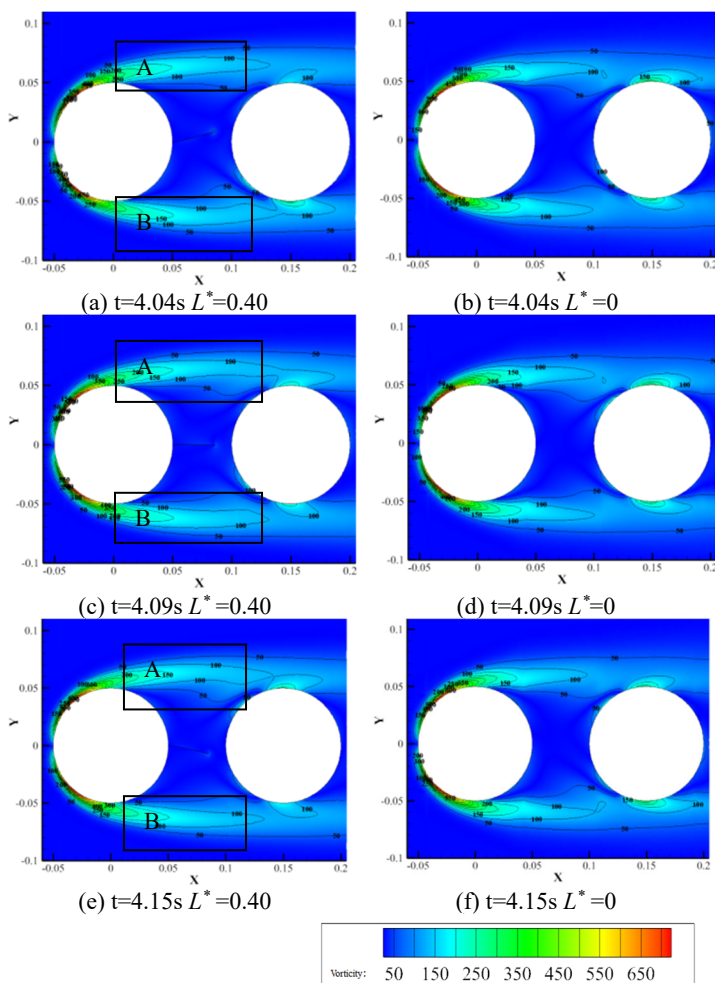


Fig. 8 $L^*=0$ and 0.40 Vorticity at different times

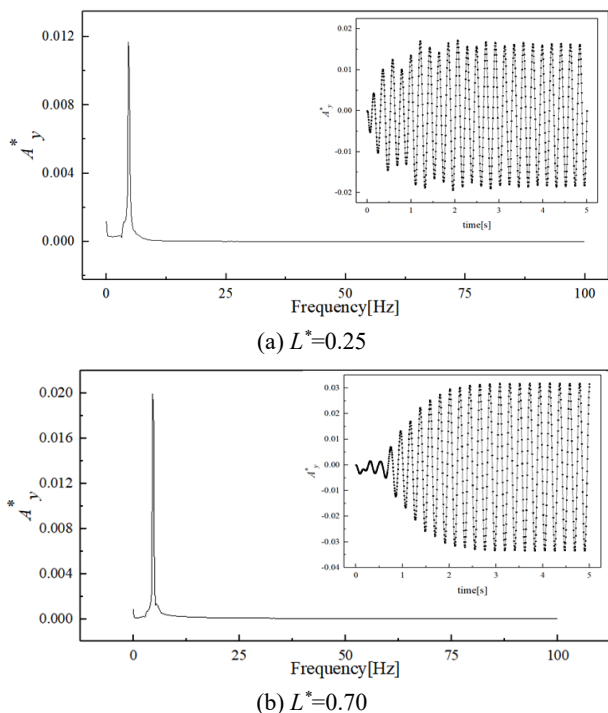


Fig. 9 $L^*=0.25$ and 0.70 A_y^* change with time and the Fourier analysis results

Under $S^*=2.0$, the trend of Nu_α while α changed is shown in Fig. 11. It is obvious that when $L^*=0.25$, Nu_α at any α is greater than $L^*=0$. The Fig.11 describes the flapping of the reed for a period the temperature gradient at different times. It can be seen from Fig.11, the flow between the tubes without the reed is basically in the symmetrical. There are obvious vortices between the cylinders, and symmetrical twin vortices appear. But when $L^*=0.25$, the disturbance between the cylinders increases, which strengthens the mixing of the fluid between the cylinders and the main fluid. Comparing Fig. 13 the temperature gradient graph at $L^*=0.70$ with Fig.12, after the length of the reed increases, the flapping amplitude increases. And because the existence of the reed hinders the mixing of the upper and lower parts fluid of the reed, the range of the dead zone increases, and the heat transfer of the downstream circular pipe is inhibited.

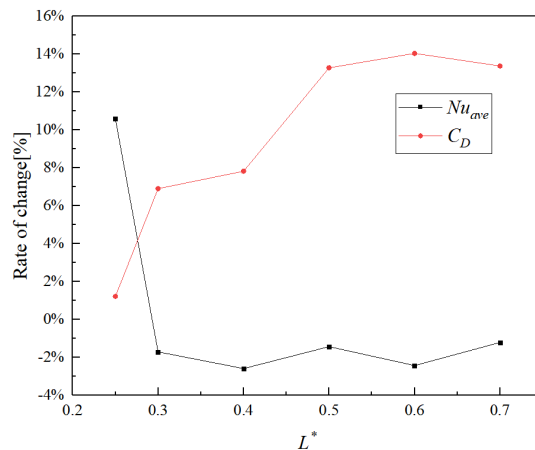


Fig. 10 Under $S^*=2.0$ trend of Nu_{ave} and C_D when the L^* changes

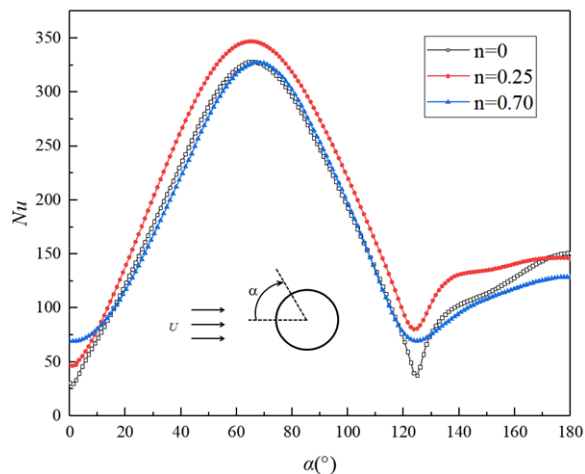


Fig. 11 $L^*= 0, 0.25$ and 0.70 Variation trend of Nu_α with α

5. CONCLUSION

In this paper, a two-dimensional numerical simulation study of the effect of a flapping reed installed between the cylinders on the heat transfer and fluid flow effect is carried out. Mainly analyze the influence of the periodic flapping of the reed with different cylinder spacing and different length on the flow field and the heat transfer of the downstream cylinder. The result shows:

1) When the cylinder spacing $S^*=1.5$ is small, as the length of the reed increases from $L^*=0.10$ to 0.40 , the heat transfer performance of the downstream cylinder is continues to increase. At this time, due to the small distance between the cylinders, there is a stable twin vortex between them, and the left side of the downstream cylinder is the front

stagnation point. After reed is added, the thermal boundary layer on the left side of the cylinder is destroyed, the degree of confusion of the fluid near the surface is increased and the heat transfer performance is enhanced.

2) In the case of the cylinder spacing $S^*=2.0$ as the length of the reed increases from 0.10 to 0.70, the heat transfer performance of downstream cylinder continues to decrease until similar to clean cylinder. When the length of the reed is small, the flapping of the flexible body increases the disturbance between the cylinders. However, with the length increases, the reed hinders the flow of the upper and lower parts of itself. Eventually lead to the dead zone area is increased, and the heat transfer of the downstream cylinder is suppressed.

3) Due to the existence of flapping reed, the stagnation point at the front point the downstream cylinder is destroyed, and the heat transfer performance is significantly increased.

4) When the cylinder spacing $S^*=2.0$, as the length of the reed increases, the domain C_D gradually increase. Due to existence of the reed, suppress fluid mixing between cylinders.

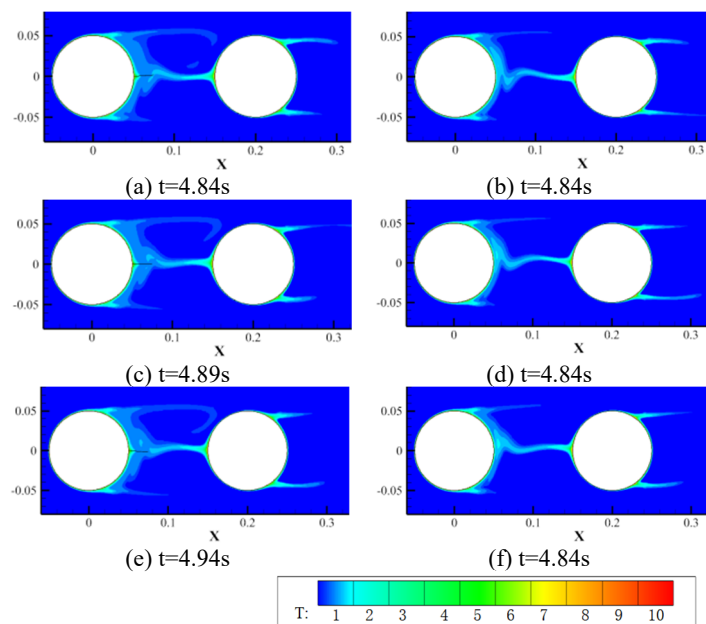


Fig.12 $L^*=0$ and 0.25 temperature gradient at different times

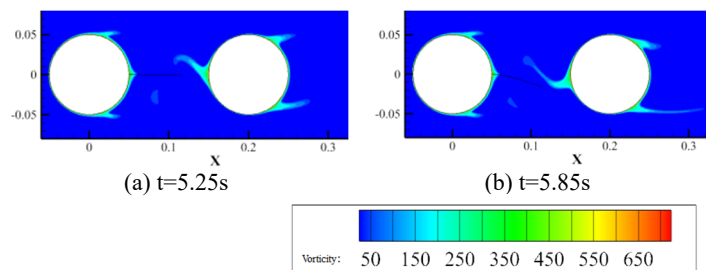


Fig. 13 $L^*=0.70$ temperature gradient at different times

NOMENCLATURE

A	amplitude (m)
C_p	specific heat (J/(kg·K))
C_L	domain length (m)
C_H	domain height (m)
D	diameter of the cylinder (m)
d	displacements(m)
E	Young's modulus (Pa)
H	reed thickness (m)

h	convection heat transfer coefficient(W/(m ² ·K))
L	reed length (m)
S	cylinders spacing (m)
T	temperature (K)
t	time (s)
U	fluid velocity(m/s)
<i>Greek Symbols</i>	
ρ	density (kg/m ³)
λ	thermal conductivity(W/(m·K))
<i>Superscripts</i>	
*	dimensionless parameters
<i>Subscripts</i>	
f	fluid
s	solid

REFERENCES

- Bergles, E., 2007, "The imperative to enhance heat transfer," *Springer Netherlands*, 13-29.
https://doi.org/10.1007/978-94-015-9159-1_2
- Beskok, A., Raisee, M., Celik, B., Yagiz, B., and Cheraghi, M., 2012, "Heat transfer enhancement in a straight channel via a rotationally oscillating adiabatic cylinder," *International Journal of Thermal Sciences*, **58**, 61-69.
<https://doi.org/10.1016/j.ijthermalsci.2012.03.012>
- Connell, B. S. H., and Yue, D. K. P., 2007, "Flapping dynamics of a flag in a uniform stream," *Journal of Fluid Mechanics*, **581**, 33-67.
<https://doi.org/10.1017/S0022112007005307>
- Chen, Y., Yang, J., Liu, Y., and Sung, H. J., 2020, "Heat transfer enhancement in a poiseuille channel flow by using multiple wall-mounted flexible flags," *International Journal of Heat and Mass Transfer*, **163**, 120447.
<https://doi.org/10.1016/j.ijheatmasstransfer.2020.120447>
- Fiebig, M., Valencia, A., and Mitra, N. K., 1993, "Local Heat Transfer and Flow Losses in Fin-Tube Heat Exchangers with Vortex Generators: A Comparison of Round and Flat Tubes," *Experimental Thermal & Fluid Science*, **8**(2), 35-45.
[https://doi.org/10.1016/0894-1777\(94\)90071-X](https://doi.org/10.1016/0894-1777(94)90071-X)
- Facchinetti, M. L., Langre, E. D., and Biolley, F., 2004, "Coupling of structure and wake oscillators in vortex-induced vibrations," *Journal of Fluids and Structures*, **19**(2), 123-40.
<https://doi.org/10.1016/j.jfluidstructs.2003.12.004>
- Gallegos, Ralph, K. B., and Sharma, R. N., 2017, "Flags as vortex generators for heat transfer enhancement: Gaps and challenges," *Renewable and Sustainable Energy Reviews*, **76**, 950-962.
<https://doi.org/10.1016/j.rser.2017.03.115>
- Khan, W. A., Culham, J. R., and Yovanovich, M. M., 2006, "Convection heat transfer from tube banks in crossflow: Analytical approach," *International Journal of Heat and Mass Transfer*, **49**(25), 4831-4838.
<https://doi.org/10.1016/j.ijheatmasstransfer.2006.05.042>
- Khanafar, K., ALAMIRI, A., and POP, I., 2010, "Fluid-structure interaction analysis of flow and heat transfer characteristics around a flexible microcantilever in a fluidic cell," *International Journal of Heat and Mass Transfer*, **53**(9-10), 1646-1653.
<https://doi.org/10.1016/j.ijheatmasstransfer.2010.01.029>
- Lee, J. B., Park, S. G., Kim, B., Ryu, J., and Sung, H. J., 2017, "Heat transfer enhancement by flexible flags clamped vertically in a Poiseuille channel flow," *International Journal of Heat and Mass Transfer*, **107**, 391-402.
<https://doi.org/10.1016/j.ijheatmasstransfer.2016.11.057>

Lee, J. B., Park, S. G., and Sung, H. J., 2018, "Heat transfer enhancement by asymmetrically clamped flexible flags in a channel flow," *International Journal of Heat and Mass Transfer*, **116**, 1003-1015.

<https://doi.org/10.1016/j.ijheatmasstransfer.2017.09.094>

Li, Z., Xu, X. C., Li, K. J., Chen, Y. Y., Huang, G. L., Chen, C. L., and Chen, C. H., 2018, "A flapping vortex generator for heat transfer enhancement in a rectangular airside fin," *International Journal of Heat and Mass Transfer*, **118**, 1340-1356.

<https://doi.org/10.1016/j.ijheatmasstransfer.2017.11.067>

Marsters, G. F., 1972, "Arrays of heated horizontal cylinders in natural convection," *International Journal of Heat & Mass Transfer*, **15**(5), 921-933.

[https://doi.org/10.1016/0017-9310\(72\)90231-1](https://doi.org/10.1016/0017-9310(72)90231-1)

Pourgholam, M., Izadpanah, E., Motamedi, R., and Habibi, S. E., 2015. "Convective heat transfer enhancement in a parallel plate channel by means of rotating or oscillating blade in the angular direction," *Applied Thermal Engineering*, **78**(78), 248-257.

<https://doi.org/10.1016/j.applthermaleng.2014.12.057>

Sohankar, A., 2007, "Heat transfer augmentation in a rectangular channel with a vee-shaped vortex generator," *International Journal of Heat and Fluid Flow*, **28**(2), 306-317.

<https://doi.org/10.1016/j.ijheatfluidflow.2006.03.002>

Song, K. W., and Wang, L. B., 2013, "The Effectiveness Of Secondary Flow Produced by Vortex Generators Mounted on Both Surfaces of the Fin to Enhance Heat Transfer in a Flat Tube Bank Fin Heat Exchanger," *Journal of Heat Transfer*, **135**(4), 041902.

<https://doi.org/10.1115/1.4023037>

Turek, S., and Hron, J., 2006, "Proposal for Numerical Benchmarking of Fluid-Structure Interaction between an Elastic Object and Laminar Incompressible Flow," *Springer Berlin Heidelberg*, 371-385.

https://doi.org/10.1007/3-540-34596-5_15

Tian, F. B., Dai, H., Luo, H., Doyle, J. F., and Rousseau, B., 2014, "Fluid-structure interaction involving large deformations: 3D simulations and applications to biological systems," *Journal of Computational Physics*, **258**, 451-469.

<https://doi.org/10.1016/j.jcp.2013.10.047>

Yoo, S. Y., Park, D. S., and Chung M. H., 2002, "Heat Transfer Enhancement For Fin-Tube Heat Exchanger Using Vortex Generators," *Journal of Mechanical Science and Technology*, **16**(1), 109-115.

<https://doi.org/10.1007/BF03185161>